

PHOTOPRODUCTION OF ELECTRON AND MUON PAIRS ON ELECTRONS

G. I. KOPYLOV, L. A. KULYUKINA, and I. V. POLUBARINOV

Joint Institute for Nuclear Research

Submitted to JETP editor September 12, 1963

J. Exptl. Theoret. Phys. (U.S.S.R.) 46, 1715-1721 (May, 1964)

The cross section for photoproduction of electron-positron and $\mu^+\mu^-$ pairs on electrons is calculated by the random-star method without neglecting any terms. All eight third-order diagrams for the process $\gamma e^- \rightarrow e^- e^- e^+$ are taken into account. The calculation has been made for the intermediate range of photon energies up to $60 m_e$, in which there are no approximate formulas. An analysis of the data from the computation enables us to determine the domain of applicability of some arguments which facilitate the derivation of approximate formulas.

THE photoproduction of electron-positron pairs on electrons has been calculated repeatedly.^[1-5] There are contributions to this process from eight diagrams; four of them are shown in Fig. 1, and in the other four electron lines 1 and 2 are interchanged. Therefore the calculation involves extremely cumbersome algebraic work, and this has never been carried through to a manageable final formula without making any approximations.¹⁾ Usually one either includes all eight diagrams but considers only limiting cases, or else neglects some of the diagrams from the beginning. Reviews of the subject^[4] concern themselves with comparisons between the various approximations, without any information being available as to how far they are from the correct result. Meanwhile, in the ultraviolet limit and with neglect of large recoil momenta some confirmation from experimental results has been obtained,^[5] since in this case one can neglect half of the diagrams (the term M_1 in Fig. 1, which gives the so-called γe interaction).

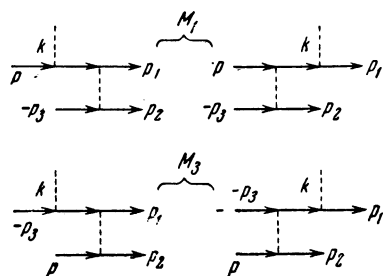


FIG. 1

¹⁾The exact expression for the cross section, not integrated over four variables, takes up four pages in the paper of Votruba.^[2]

The calculation is most difficult in the intermediate region, in which none of the diagrams can be neglected. We decided to make use of the possibility provided by the method of random stars,^[6] and have calculated the process of photoproduction of e^+e^- pairs in this region in the Born approximation with a computing machine, without any approximations. The results of the computations give the behavior of the cross section in the range of values of the photon energy k (in the laboratory system) $4.01-60 m_e$, in which the known analytic formulas do not "work," and indicate the energies for which the considerations on which the derivations of these approximate formulas are based become legitimate.

1. THE BASIC FORMULA AND THE METHOD OF CALCULATION

The variables chosen to describe the state of the system of two electrons 1 and 2 and the positron 3 were: the kinetic energy τ_2 of the pair 1+2 and the direction of particle 2 in the rest system of the pair 1+2; the direction of particle 3 in the rest system of 1+2+3; the spin indices of all the particles. These variables were taken to be distributed randomly and uniformly over their ranges of variation. It is important that for none of these variables does the range of variation depend on the other variables.^[7] Calculating with the values of the five variables in the momentum space of the rectangular components of the momenta of all three particles, we could get explicit numerical expressions for the elements of the matrices—the propagation functions and column and row factors—of the electron and positron wave functions. The choice of a particular column (or row) was

dictated by the result of a random choice of the spin variables. Then by direct matrix multiplication the value of the amplitude for the process was computed for the given choice of the state variables. The weighted average of the square of the absolute value of the amplitude over some number N of randomly chosen states ("random stars") gave the cross section

$$\sigma = \frac{1}{N} \sum_{\lambda=1}^N \Phi^{(\lambda)}.$$

The formula for calculating the weight $\Phi^{(\lambda)}$ of a randomly chosen state λ was of the form $\Phi = KF$, where the factor K contained the Jacobian of the transformation from the variables p_1, p_2, p_3 to the variables used here, and factors from the integration of the δ function in the expression for the cross section and from division by the flux of photons. $F = |M|^2$, where $M = M_1 - M_2 - M_3 + M_4$ is the sum of the amplitudes for the processes represented by pairs of diagrams (only M_1 and M_3 are shown in Fig. 1).

As an example we write out M_1 :

$$M_1 = -\frac{e^3}{\sqrt{2k}} (\bar{u}_1 V_\nu u) \frac{1}{\Delta^2} (\bar{u}_2 \gamma_\nu v_3), \quad (1)$$

$$V_\nu = \gamma_\nu \frac{-i(\hat{k} + \hat{p}) + m}{(k+p)^2 + m^2} \hat{\varepsilon}(k) + \hat{\varepsilon}(k) \frac{-i(\hat{p}_1 - \hat{k}) + m}{(p_1 - k)^2 + m^2} \gamma_\nu, \quad (2)$$

$$\Delta = p_2 + p_3; \quad (3)$$

Here one takes as $\hat{\varepsilon}$ either γ_1 or γ_2 , depending on which of the two polarization states of the photon is selected at random. The wave functions \bar{u}_1 and \bar{u}_2 for creation of electrons 1 and 2 are of the form given by the matrix row

$$\frac{1}{\sqrt{8}} \left\{ \frac{\sqrt{1 \pm c}}{\sqrt{1 \pm v}} (1 \pm v + \gamma^{-1}); \pm (a - ib) \frac{1 \pm v + \gamma^{-1}}{\sqrt{1 \pm c} \sqrt{1 \pm v}}; \right. \\ \left. - \frac{\sqrt{1 \pm c}}{\sqrt{1 \pm v}} (1 \pm v - \gamma^{-1}); \mp (a - ib) \frac{1 \pm v - \gamma^{-1}}{\sqrt{1 \pm c} \sqrt{1 \pm v}} \right\}, \quad (4)$$

with the upper or lower signs, depending on the random selection of the sign of the spin projection (helicity); here a, b, c are the direction cosines of the velocity of the electron and γ is its relativistic factor.

As the wave function v_3 for the creation of the positron one uses a matrix column with the same elements, but with the opposite signs for the quantities a, b, c, v, γ^{-1} . As the wave function u of the electron that is annihilated (the target) one uses the elements of one of the two columns $u(p, \pm \frac{1}{2})$:

$$u\left(p, -\frac{1}{2}\right) = \begin{pmatrix} 0 \\ \frac{1+v+\gamma^{-1}}{2\sqrt{1+v}} \\ 0 \\ \frac{1+v-\gamma^{-1}}{2\sqrt{1+v}} \end{pmatrix}; \quad u\left(p, \frac{1}{2}\right) = \begin{pmatrix} -\frac{1-v+\gamma^{-1}}{2\sqrt{1-v}} \\ 0 \\ -\frac{1-v-\gamma^{-1}}{2\sqrt{1-v}} \\ 0 \end{pmatrix}. \quad (5)$$

Finally, the propagator factor $-\hat{p} + m$, where $p = \{x, y, z, E\}$, was in the form of the matrix

$$\begin{pmatrix} E+m & 0 & -z & -x+iy \\ 0 & E+m & -x-iy & z \\ z & x-iy & -E+m & 0 \\ x+iy & -z & 0 & -E+m \end{pmatrix}. \quad (6)$$

The calculation of M_2, M_3, M_4 was made with the same formulas as that of M_1 , but the arguments of the propagators and wave functions were rearranged to correspond with the changes of the lines in the pairs of diagrams that give M_2, M_3, M_4 . The simplicity of the logical operation eliminated the possibility of error in this part of the calculation, which was the most complicated from the analytical point of view.

In the cross-section calculations we confined ourselves to an averaging over 1000 random stars, which required one and one-half hours of machine time. The degree of approximation was estimated by the machine itself from the average spread of the weights of these stars. The spread was determined by the nonuniformity of the distribution of the weights of the states in phase space. With our choice of the variables of integration this nonuniformity was small for photon energies $k \leq 10 m_e$, and above this it increased rapidly, which hindered accurate calculations. Therefore we calculated the cross sections by this method only in the energy range up to $10 m_e$. We emphasize that this is not the nonrelativistic limit; for the process $\gamma e^- \rightarrow e^- e^- e^+$ this latter limit does not exceed $4.01 m_e$, with the threshold at $4 m_e$.

Together with the averaging of the weights of the states over the entire phase space an averaging was carried out over parts of the phase space located between level surfaces of various functions of the state variables. In this way, in parallel with the calculation of the cross section we calculated distributions with respect to ten quantities: the momenta and angles of emergence of e^+ and e^- , the angle between e^+ and e^- , the effective masses of the pairs $e^- e^-$ and $e^- e^+$, and the quantities $\eta_1 = \omega_- / (\omega_- + \omega_+)$ and $\eta_2 = \omega_-^{(1)} / (\omega_-^{(1)} + \omega_-^{(2)})$ —the fractions of the total energies of the $e^- e^+$ and $e^- e^-$ pairs that go to the e^- . The histograms so obtained were not accurate enough (~ 20 percent), however,

and we reduced each of them to a single characteristic quantity—the average value of the quantity in question.

For the calculation of the cross sections for $k > 10 m_e$ we made use of the fact that in the ultra-violet limit the main contribution to the cross section comes from configurations with small momentum transfers $(p - p_2)^2$ and $(p - p_1)^2$ (the terms M_3 and M_4). Therefore one must go over to a phase space in which level values of the pole expression

$$A = \frac{d^3 p_1 d^3 p_2 d^3 p_3}{\omega_1 \omega_2 \omega_3} \frac{1}{(p - p_1)^4} \delta^4(p_1 + p_2 + p_3 - k - p) \quad (7)$$

are used.

This can be done if we define the absolute value of the momentum p_2 and the direction $\bar{\varphi}_2, \bar{\theta}_2$ of particle 2 in the rest system of 1+2 and the direction φ_1, θ_1 of particle 1 in the rest system of 1+2+3 by means of the equations

$$\int_0^{\bar{p}_2} \frac{\bar{p}_2^2 p_1}{M_2 (\omega_p - \omega_1)^2} dp_2 = r_1 \int_0^{\bar{p}_2 \max} \frac{\bar{p}_2^2 p_1}{M_2 (\omega_p - \omega_1)^2} dp_2 \equiv r_1 J,$$

$$\omega_p = (p^2 + m_e^2)^{1/2}, \quad M_2 = 2(\bar{p}_2^2 + m_e^2)^{1/2},$$

$$M_3^2 = -(k + p)^2, \quad (8)$$

$$\omega_1 = \frac{M_3^2 + m_e^2 - M_2^2}{2M_3}, \quad p_1 = (\omega_1^2 - m_e^2)^{1/2},$$

$$\bar{p}_{2 \max} = \frac{M_3^2 + m_e^2 - (2m_e)^2}{2M_3}.$$

$$\cos \theta_1 = \frac{2(-m_e^2 - \omega_p \omega_1) r_2 - (-m_e^2 + \omega_p \omega_1 - p p_1)}{(-m_e^2 + \omega_p \omega_1 - p p_1) + 2p p_1 r_2},$$

$$\varphi_1 = 2\pi r_3, \quad \bar{\varphi}_2 = 2\pi r_4, \quad \cos \bar{\theta}_2 = -1 + 2r_5. \quad (9)$$

Then in the new variables r_1, \dots, r_5 points with the density (7) are distributed uniformly in the five-dimensional cube, so that

$$A = \frac{16 \pi^2}{M_3 m_e^2} J d^5 r, \quad (10)$$

and the "weight" of a state characterized by the vector \mathbf{r} and a set of spin variables takes the form

$$\Phi = \frac{4 \cdot 32}{137^3} \frac{\omega_1 \omega_2 \omega_3}{k M_3 m_e^2} J |M|^2 (p - p_1)^4. \quad (11)$$

In the nonrelativistic region this choice of variables reduces to the one used before; in the ultra-relativistic region it decreases the cross section by a factor two, since it selects events only in the region with small $(p - p_1)^2 + m_e^2$, and no events with small $(p - p_2)^2 + m_e^2$ are encountered in this way. To remove this indefiniteness in the coefficient, in the computation cases with $|(p - p_2)^2| < |(p - p_1)^2|$ were simply omitted, and the result given by the machine was multiplied by two.

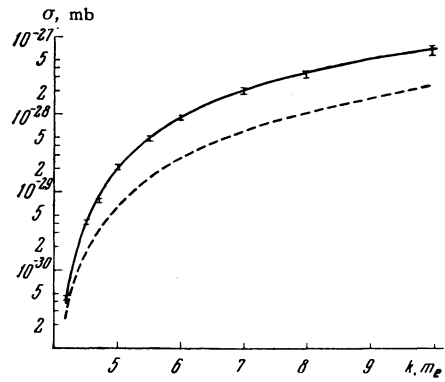


FIG. 2. Cross section for the process $\gamma e^- \rightarrow e^- e^- e^+$. The solid curve was calculated by the method of random stars; the dashed curve, by the nonrelativistic formula.

2. RESULTS

Figure 2 shows the cross section for the process $\gamma e^- \rightarrow e^- e^- e^+$ in the range $4 < k/m_e \leq 10$. For comparison we show the curve of the formula usually used to calculate the cross section in this range—the nonrelativistic formula of Votruba^[2,4]:

$$\sigma = a r_0^2 \frac{\pi \sqrt{3}}{2 \cdot 3^5} \left(\frac{k}{m_e} - 4 \right)^2 = 6.52 \cdot 10^{-30} \left(\frac{k}{m_e} - 4 \right)^2 \text{cm}^2. \quad (12)$$

The curves coincide only up to $4.01 m_e$, and differ in the rest of the range by a factor of 2–3.5. The error in the determination of the cross section by the method of random stars increases from 5 percent at the threshold to 10 percent at $10 m_e$.

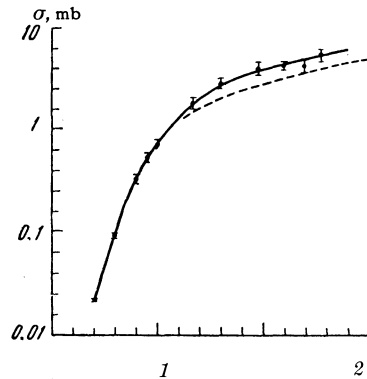


FIG. 3. Cross section for the process $\gamma e^- \rightarrow e^- e^- e^+$ in the range of energies k up to $60 m_e$; the dashed curve is from the Bethe-Heitler formula. The abscissa is the quantity $\log(k/m_e)$.

Figure 3 shows the behavior of the cross section in the range up to $60 m_e$ along with, for comparison, the curve calculated from the ultrarelativistic formula of Bethe and Heitler for photoproduction on a Coulomb center of force:

$$\sigma = a r_0^2 \left(\frac{28}{9} \ln \frac{2k}{m_e} - \frac{218}{27} \right)$$

$$= 4.49 \cdot 10^{-27} \left(\log \frac{2k}{m_e} - 1.126 \right) \text{cm}^2 \quad (13)$$

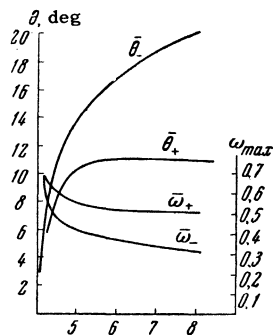


FIG. 4. Dependences of the mean angle of emergence θ and the mean energy ω of electron (-) and positron (+) in the laboratory reference system on k/m_e . ω_{max} is the maximum energy of the electron allowed by the kinematics.

Beginning at about $50 m_e$ this formula reproduces the cross section for the process rather well.

Other indications that the ultrarelativistic formula can be used appear even earlier. Figures 4 and 5 show how the mean angles of emergence and the mean energies of e^- and e^+ depend on the photon energy in various ranges of k . On the average e^+ has a larger energy and emerges at a smaller angle than e^- . Evidently, already at energies of the order of $60 m_e$ the photoproduction is determined by the last two diagrams (and the diagram with electrons 1 and 2 interchanged), as is the case at extremely high energies. According to these diagrams, the particles of the e^+e^- pair must retain in the center-of-mass system the backward motion of the target electron. Therefore in the laboratory system it must have a smaller energy and a larger angle of emergence than the members of the e^+e^- pair.

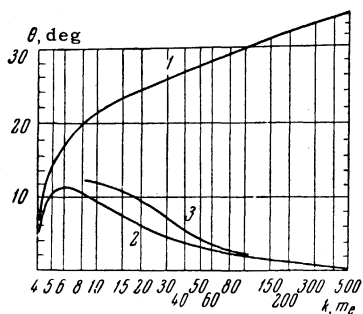


FIG. 5. Dependences of mean angles of emergence in the laboratory reference system on the photon energy in the range up to $500 m_e$: 1 - for the electrons, 2 - for the positrons, 3 - for the fast electrons only.

Already at $k \sim 10 m_e$ one can easily distinguish the electrons from each event as a fast electron with energy $\sim k/2$ and a slow one with total energy $1.2-2 m_e$, and their angular distribution becomes an obviously two-lobed one (Fig. 5). These electrons can be regarded as not identical—they are

marked by their speeds—and we can neglect the interference between the diagrams that differ by the interchange of particles 1 and 2. The cross section for the process represented by the four pole diagrams $M_3 M_4$ is equal to twice that of the process represented by the two diagrams M_3 . In these diagrams, however, we can neglect reversals of the spin of the target electron. The calculation showed that the ratio of the contributions to the cross section from events with reversal of the spin of the target electron after the interaction to that from events without such reversal is 7–8 percent at $k = 9-15 m_e$, 1 percent at $30-50 m_e$, 0.2 percent at $100 m_e$. This is closely connected with the small momentum transfer $(p - p_2)^2$ to the target, and means that at the bottom vertex of the remaining diagrams there is essentially a nonrelativistic scattering of the electron at a Coulomb center. These considerations are well known^[4]; our calculations show at what energies they begin to be valid.

This picture of the interaction is confirmed by the fraction of the total energies of e^+e^- and e^-e^- pairs that goes to one electron. At large k this quantity η varies practically uniformly from zero to unity, with a small decrease of the frequency at the extreme values of η .^[5] In the nonrelativistic limit, on the other hand, $\eta = 1/2$, and as k increases the limits between which η varies become wider (Fig. 6). As is shown by the distribution in η (shown for $k = 6 m_e$ in Fig. 6), the energy of e^- in a pair e^-e^+ is on the average less than half of the total energy of the pair. Also, however, two electrons have unequal energies more often than equal.

The distributions of the effective masses m_{-} and m_{+} of pairs e^-e^- and e^+e^- do not show any

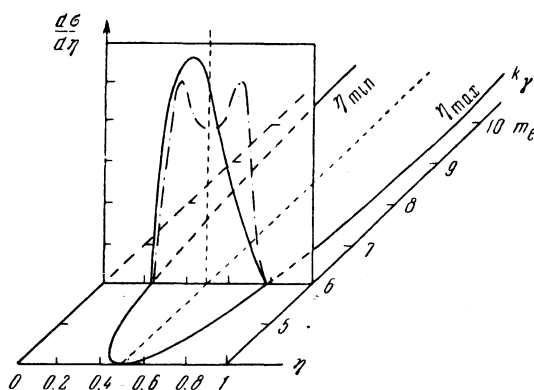


FIG. 6. Dependence of the range of variation of the quantity η on the photon energy, and a typical distribution in η in the intermediate region of photon energies. The solid curve is $d\sigma/d\eta$ with $\eta = \omega_-/(\omega_- + \omega_+)$; the dot-dash curve is $d\sigma/d\eta$ with $\eta = \omega_-/(\omega_-^{(1)} + \omega_-^{(2)})$.

characteristic differences from the distributions calculated with the matrix element set equal to unity. For energies $k < 10 m_e$, however, the average value of $m_{-} - 2m_e$ is approximately 0.55 of the kinetic energy of all three particles in the center-of-mass system, whereas the average value of $m_{+} - 2m_e$ is 0.46 of this quantity.

The similarity of the diagrams for the processes $\gamma e^- \rightarrow e^- e^- e^+$ and $\gamma e^- \rightarrow e^- \mu^- \mu^+$ allowed us to calculate also the cross section for the latter process (we had only to set $M_2 = M_4 = 0$ in the formula $F = |M|^2$). In the range of energies chosen (45–55 BeV) the accuracy of the calculation was already low (Fig. 7) and did not allow a more detailed analysis of the conditions for detecting this as yet unobserved process of the production of muon pairs on electrons.

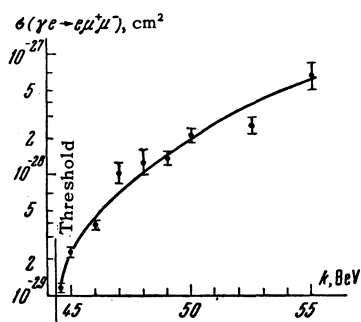


FIG. 7

These first test calculations by the new method (see also [8]) enable us to draw some preliminary conclusions about its domain of applicability. For processes represented by four to eight third-order diagrams this method gives in 1–1.5 hours an accuracy of 5–10 percent in the determination of cross sections. This is not so bad if we consider that the approximations that are unavoidable in the derivation of analytic formulas can affect the result by as much as 300 percent. The method works

well in the nonrelativistic and intermediate energy ranges, but when the poles of the amplitude approach the physical region—i.e., in the ultrarelativistic limit—it requires that the singularities of the amplitude be taken into account, or else the error rapidly increases. In just the same way, the error increases when there are sharp form-factors. This difficulty is not one of principle and can be removed by an appropriate choice of the variables of integration.

The authors thank M. A. Markov for his interest in this work, and B. N. Valuev for valuable discussions.

¹H. A. Bethe and W. Heitler, Proc. Roy. Soc. **A146**, 83 (1934).

²V. Votruba, Phys. Rev. **73**, 1468 (1948); Bull. Intern. Acad. Tcheque Sci. **49**, 19 (1948).

³J. A. Wheeler and W. E. Lamb, Jr., Phys. Rev. **55**, 858 (1939); **101**, 1836(E) (1956). A. Borsellino, Nuovo cimento **4**, 112 (1947). K. M. Watson, Phys. Rev. **72**, 1060 (1947). P. É. Nemirovskii, JETP **10**, 893 (1948). B. K. Fedyushin, JETP **22**, 140 (1952).

⁴J. Joseph and F. Rohrlich, Revs. Modern Phys. **30**, 354 (1958).

⁵K. S. Suh and H. A. Bethe, Phys. Rev. **115**, 672 (1959). Hart, Cocconi, Cocconi, and Sellen, Phys. Rev. **115**, 678 (1959).

⁶G. I. Kopylov and I. V. Polubarinov, Joint Inst. for Nuclear Research Preprint D-821 (1961).

⁷G. I. Kopylov, JETP **39**, 1091 (1960), Soviet Phys. JETP **12**, 761 (1961); Dissertation, ITÉF, 1962.

⁸Kopylov, Polubarinov, and Semashko, JETP **46**, 1320 (1964), Soviet Phys. JETP **19**, 894 (1964).

Translated by W. H. Furry